Original Article

Feasibility study of low-dose computed tomography (CT) technology for maxillofacial bone three-dimensional (3D) printing in skeletal class III malocclusion

Qian Miao[1], Guan Li[2]^, Yì Xiáng J. Wáng[3], Jinbao Wang[4], Haopeng Wang[4], Wei Chen[5], Yang Shao[6]

[1]Department of Anesthesiology, Jinling Hospital, Affiliated Hospital of Medical School, Nanjing University, Nanjing, China; [2]Department of Radiology, Nanjing Drum Tower Hospital, Affiliated Hospital of Medical School, Nanjing University, Nanjing, China; [3]Department of Imaging and Interventional Radiology, Prince of Wales Hospital, the Chinese University of Hong Kong, Shatin, Hong Kong SAR, China; [4]Department of Radiology, General Hospital of Northern Theater Command, Shenyang, China; [5]Department of Stomatology, Jinling Hospital, Affiliated Hospital of Medical School, Nanjing University, Nanjing, China; [6]Department of Stomatology, General Hospital of Northern Theater Command, Shenyang, China

Contributions: (I) Conception and design: Q Miao, G Li; (II) Administrative support: J Wang, H Wang; (III) Provision of study materials or patients: G Li, Y Shao; (IV) Collection and assembly of data: W Chen; (V) Data analysis and interpretation: Y Shao, W Chen; (VI) Manuscript writing: All authors; (VII) Final approval of manuscript: All authors.

Correspondence to: Wei Chen, MD. Department of Stomatology, Jinling Hospital, Affiliated Hospital of Medical School, Nanjing University, 305 Zhongshan East Road, Xuanwu District, Nanjing 210002, China. Email: rollphy@aliyun.com; Yang Shao, MD. Department of Stomatology, General Hospital of Northern Theater Command, 83 Wenhua Road, Shenhe District, Shenyang 110016, China. Email: shaoyang8306@163.com.

Background: Skeletal class III malocclusion is among the most common dental and maxillofacial malformations. Three-dimensional (3D) printing technology has become widely applied in orthopaedics. The data source for 3D printing of maxillofacial bones is computed tomography (CT). The issue of the CT radiation dose caused by maxillofacial bone 3D printing has attracted increasing attention. This study aimed to explore the feasibility of low-dose CT technology in maxillofacial bone 3D printing and the clinical value of low-dose maxillofacial bone 3D printing.

Methods: Ninety patients with class III malocclusion who planned to undergo maxillofacial bone 3D printing and 3D-CT were prospectively enrolled and randomly divided into the conventional CT dose 3D printing group (Group A, n=28), low-CT dose 3D printing group (Group B, n=32) and 3D-CT control group (Group C, n=30). The quality of maxillofacial bone 3D printing was subjectively evaluated, and a Likert-scale questionnaire was used to assess the clinical value of maxillofacial bone 3D printing.

Results: No significant differences in the general demographic characteristics were detected among Groups A, B, and C. Compared with that in Group A (0.8±0.1 mSv), the radiation effective dose (ED) in Group B (0.3±0.1 mSv) was reduced by approximately 63%. There were no significant differences between Groups A and B in 3D printing quality indices (including clarity, integrity, accuracy or artefacts) (all P>0.05). There were significantly higher subjective scores for the clinical value of maxillofacial bone 3D printing (Group A=4.1±0.5, 4.0±0.5, 4.0±0.4 and 4.1±0.5; Group B=4.0±0.5, 4.0±0.4, 4.0±0.5 and 4.0±0.5) than for 3D-CT (Group C=3.1±0.5, 3.1±0.4, 2.9±0.4 and 3.0±0.4) in diagnosing and classifying, formulating the surgical plan, simulating the surgical process, and predicting postoperative recovery (all P<0.05).

Conclusions: Low-dose CT technology can be effectively applied for maxillofacial bone 3D printing, reducing the radiation dose without affecting the 3D printing quality. Maxillofacial bone 3D printing technology is superior to 3D-CT in class III malformations.

^ ORCID: 0000-0002-3353-993X.

Keywords: Three-dimensional printing (3D printing); low-dose; computed tomography (CT); maxillofacial bone; class III malocclusion

Submitted Nov 16, 2022. Accepted for publication Aug 27, 2024. Published online Oct 17, 2024.
doi: 10.21037/qims-22-1266
View this article at: https://dx.doi.org/10.21037/qims-22-1266

Introduction

Skeletal class III malocclusion is a common form of dental and maxillofacial malformation (incidence of approximately 14% in the Asian population) and is characterized by malocclusion caused by excessive forward growth of the mandible with or without maxillary retraction (1,2). Skeletal Class III malocclusion is divided into three subdivisions, which have different treatment schemes (3,4). Accurate preoperative typing judgement, sufficient preoperative measurement, and skilled preoperative surgical simulation are important for the treatment of class III malocclusion.

Currently, three-dimensional (3D) computed tomography (CT) is used for the preoperative evaluation of class III malocclusion; however, the results are displayed on a two-dimensional (2D) film or plane, which challenges the surgeon's sense of 3D space. Recently, 3D printing technology has been broadly applied in the medical field, showing obvious advantages in actuality, accuracy, vitality, and 3D space sense. At present, the main data source of maxillofacial bone 3D printing is digital imaging and communications in medicine (DICOM) data generated after CT scanning (5). The CT machine needs to meet the requirements of high-resolution CT scanning (scan slice thickness, 0.625 mm). To perform 3D printing of maxillofacial bones, people often overlook the issue of patients' radiation dose exposure (the CT radiation dose is often higher than the 1.0 mSv).

In recent years, low-dose CT technology has been widely used in the clinic, which involves low tube voltage, low tube current, a large pitch, a shortened exposure time, and the application of an iterative reconstruction algorithm (6,7). Low-dose CT technology often comes at the cost of reducing image quality, but in recent years, improved CT postprocessing functions and algorithms have significantly compensated for the decrease in image quality caused by low-dose CT scanning. A previous study confirmed that low-dose CT technology can reduce the radiation dose used for maxillofacial bone CT scanning by 88% without affecting the quality of the CT image (8). In the present study, our purpose was to explore the feasibility of applying low-dose CT technology to 3D printing of maxillofacial bones and further explore the clinical application value of low-dose 3D printing of maxillofacial bones in class III malocclusions. We present this article in accordance with the GRRAS reporting checklist (available at https://qims.amegroups.com/article/view/10.21037/qims-22-1266/rc).

Methods

Patient selection

Patients (n=90; 51 males and 39 females, with a median age of 45.2±13.8 years and an age range of 19–65 years) with suspected class III malocclusion who underwent maxillofacial bone 3D printing or maxillofacial bone 3D-CT at Jinling Hospital, Affiliated Hospital of Medical School, Nanjing University, China, were reviewed prospectively between January 2020 and March 2024. These patients were randomized into the conventional CT dose 3D printing group (Group A, n=28), the low-CT dose 3D printing group (Group B, n=32) and the 3D-CT control group (Group C, n=30). The study was conducted in accordance with the Declaration of Helsinki (as revised in 2013). Ethical approval for this prospective study was obtained from the Ethics Committee of Jinling Hospital, Affiliated Hospital of Medical School, Nanjing University, China (No. 2022DZGZR-075), and all patients provided informed consent to participate in the investigation.

The inclusion criteria were as follows: (I) clinically confirmed or highly suspected class III malocclusion and (II) age >18 years. The exclusion criteria were as follows: (I) metal implants that affect CT image quality and (II) severe cardiovascular disease, cerebrovascular disease, or critical illness.

DICOM data acquisition

Maxillofacial bone CT DICOM data were obtained via a Discovery CT 750 HD scanner (GE Healthcare, Milwaukee, USA). The head was fixed before examination, and the scan range was from the lower jaw to the upper eye

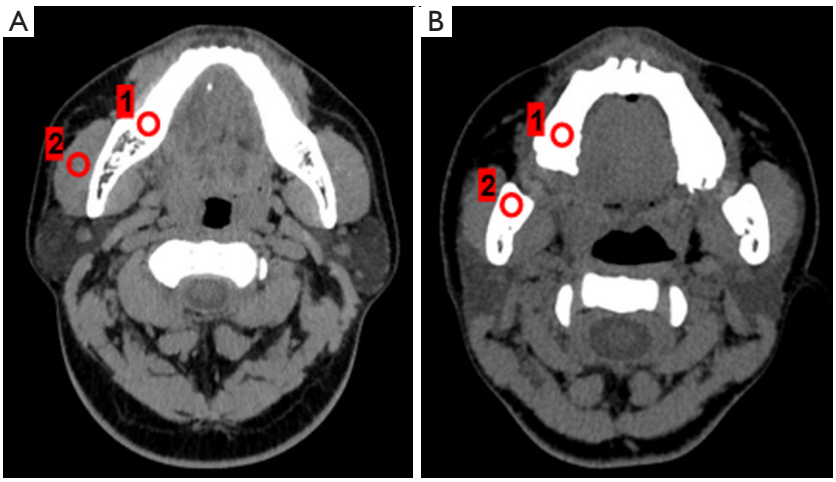

Figure 1 ROIs selected from the CT DICOM data between the Group A and Group B protocols. ROI 1, jawbone; ROI 2, masseter muscle; Group A, conventional CT dose 3D printing group; Group B, low CT dose 3D printing group. ROIs, regions of interest; CT, computed tomography; DICOM, digital imaging and communications in medicine; 3D, three-dimensional.

socket. In Group A and Group C, we used 120 kVp and 200 mA (a routine CT scanning protocol). In Group B, we used 80 kVp with automatic tube current modulation (ATCM, 50–220 mA) (a low-dose CT scanning protocol). The adaptive statistical iterative reconstruction (ASiR, GE Healthcare, Milwaukee, WI, USA) algorithm was used for Groups A, B, and C. According to previous research reports, 50% ASiR was selected (9).

The following CT scanning parameters were identical across all groups: bed speed, 39 mm/r; gantry rotation time, 0.5 s; pitch, 0.984:1; slice collimation, 40 mm; scanning field, 25 cm; and reconstruction slice thickness, 0.625 mm.

DICOM data quality evaluation

On the GE AW4.6 workstation, regions of interest (ROIs) were selected to ensure that the same target tissue was present. The ROI size was defined as a circular 1.00 cm^2 in size. The location of the ROI was selected to measure the CT value at the same level as the jawbone and masseter muscle (*Figure 1*). The standard deviation (SD) of the masseter muscle was measured as an indicator of background noise (BN).

The signal-to-noise ratio (SNR) and contrast-to-noise ratio (CNR) were calculated according to the following formulas:

$$\mathrm{SNR} = \frac{\mathrm{CT}_{\text{jaw bone}}}{\mathrm{SD}_{\text{masseter muscle}}} \quad [1]$$

$$\mathrm{CNR} = \frac{\mathrm{CT}_{\text{jaw bone}} - \mathrm{CT}_{\text{masseter muscle}}}{\mathrm{SD}_{\text{masseter muscle}}} \quad [2]$$

Radiation dose estimation

The CT dose index volume (CTDIvol), dose-length product (DLP) and Z axial scanning range were recorded. The effective dose (ED) was calculated by multiplying the DLP by a conversion factor of 0.0021 mSv/(mGy·cm) (10).

3D modelling and printing

All the CT DICOM data in Groups A and B were input into visual 3D modelling software (Visual Co., Ltd., Beijing, China). One 3D printing engineer (with 8 years of experience in 3D printing) performed the 3D modelling and 3D printing in all the cases. The automatic segmentation function was used to segment and extract the targets, such as the skull, maxillofacial bone, maxilla, and mandible. Irrelevant structures, such as the CT bed plate and metallic foreign bodies, were removed. In cases that could not be automatically segmented or had inaccurate segmentation boundaries, we chose to draw the ROIs manually. Each target was processed via expansion, corrosion, rendering, and smoothing functions and then saved as standard tessellation language (STL) files. In scene editing function mode, all STL files were imported and underwent colour, transparency, clarity, and contrast adjustments to realize the

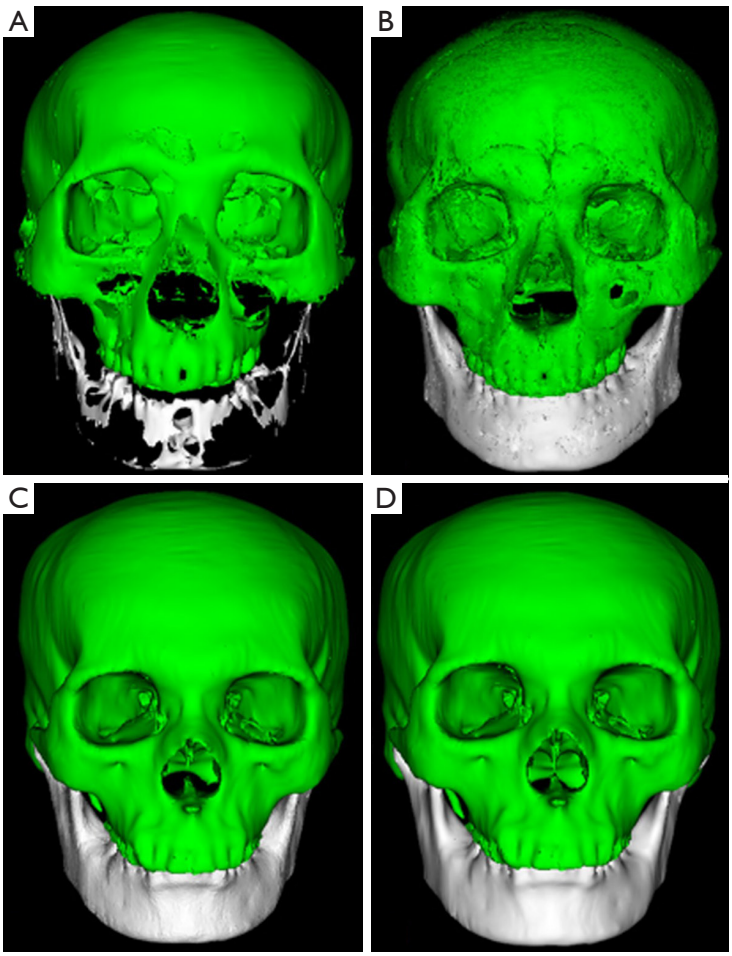

Figure 2 Maxillofacial bone 3D modelling quality evaluation on a four-point scale. (A) 1 point: the clarity is poor, a large portion of the anatomy is absent, the accuracy is unacceptable, and the artefacts are serious; the model is considered nondiagnostic. (B) 2 points: the clarity is suboptimal, a small portion of the anatomy is absent, the accuracy is fair, and many artefacts are present; the model is considered nondiagnostic. (C) 3 points: the clarity, integrity, and accuracy are good, and few artefacts are present; the model is acceptably diagnostic. (D) 4 points: the clarity and accuracy are excellent, the integrity is perfect, and almost no artefacts are present; the model is suitably diagnostic. 3D, three-dimensional.

best 3D modelling effect. A 3D rapid prototyping printer (MakerBot Replicator Z18, USA) was used to print the 3D model using acrylonitrile butadiene styrene copolymer material.

Subjective evaluation

Under double-blind conditions, without knowledge of the specific experimental protocol, two maxillofacial surgeons (with 25 and 15 years of experience) subjectively evaluated the maxillofacial bone 3D modelling and printing quality between Group A and Group B. A 4-point scale was adopted, and maxillofacial bone low-dose CT images were used as references for evaluating the quality of 3D printing (6). The main evaluation indices of 3D modelling and printing quality included clarity, integrity, accuracy, and artefacts (*Figure 2*):

(I) Clarity refers to the boundaries and tiny details of the 3D printed model, which can be affected by the quality of the DICOM data or reconstruction software properties. The clarity scoring standard was as follows: 1 point, extremely poor; 2 points, poor; 3 points, good; and 4 points, excellent.

(II) Integrity refers to the integrity of the anatomical structure, which can be affected by segmentation errors or a lack of sufficient DICOM data. The

Table 1 Clinical characteristics of the patients

Index	Group A (n=28)	Group B (n=32)	Group C (n=30)	P value
Age (years)	39.5±12.4	41.5±13.3	40.2±15.6	0.556
Height (cm)	171.6±7.1	169.9±6.0	170.4±8.4	0.325
Weight (kg)	71.7±8.9	70.5±10.6	73.1±12.9	0.391
BMI (kg/m^2)	24.2±2.0	24.3±3.0	24.9±3.0	0.434
Class III malocclusion				
Type I	12 [43]	15 [47]	14 [47]	0.761
Type II	8 [29]	11 [34]	10 [33]	0.636
Type III	8 [29]	6 [19]	6 [20]	0.386

Data are presented as mean ± standard deviation or n [%]. Group A, conventional CT dose 3D printing group; Group B, low-CT dose 3D printing group; Group C, 3D-CT control group. BMI, body mass index; CT, computed tomography; 3D, three-dimensional.

integrity scoring standard was as follows: 1 point, large part missing; 2 points, small part missing; 3 points, complete; and 4 points, perfect.

(III) Accuracy refers to the anatomical relationship and the location, scope, shape, and size of the lesions, which can be compared with those of CT images. The accuracy can be affected by the quality of the DICOM data. The accuracy scoring standard was as follows: 1 point, extremely poor; 2 points, poor; 3 points, correct; and 4 points, accurate.

(IV) Artefacts refer to abnormal 3D printed models that do not conform to the actual anatomical structure, which can be affected by the quality of the DICOM data and the reconstruction software properties. The artefact scoring standard was as follows: 1 point, serious; 2 points, moderate; 3 points, mild; and 4 points, no artefact.

A 3D modelling quality score ≥3 points was considered to meet the needs of clinical diagnosis and treatment.

Clinical value evaluation

Six maxillofacial surgeons with different levels of seniority (2 senior titles, 2 middle titles and 2 primary titles) were selected to subjectively evaluate the clinical value of maxillofacial bone 3D printing in class III malocclusion. Senior doctors were defined as having been engaged in maxillofacial plastic surgery for more than 20 years; middle doctors were defined as having been engaged in maxillofacial plastic surgery for 10–20 years; and primary doctors were defined as having been engaged in maxillofacial plastic surgery for less than 10 years. The 3D-CT results for class III malocclusions were selected as the control group. Using a Likert-scale questionnaire survey, subjective scores were given for four aspects: (I) diagnosing and classifying; (II) formulating the surgical plan; (III) simulating the surgical process; (IV) predicting postoperative recovery. The following 5-point system was adopted: 5 points, very satisfactory; 4 points, satisfactory; 3 points, neutral; 2 points, unsatisfactory; and 1 point, very unsatisfactory.

Data analysis

SPSS version 17.0 (SPSS, Inc., Chicago, IL, USA) was used for statistical analysis. Quantitative variables are reported as the mean ± SD. Categorical variables are described as frequencies or percentages. Student's *t*-test was used to compare the means of two independent samples. The χ^2 test was used to compare count data. Bonferroni-corrected P values were used to account for multiple comparisons. Correlations were analysed using the Pearson chi-square test. The linear-weighted kappa test was used to measure the consistency of the subjective scores. The interobserver agreement based on kappa values was classified as follows: ≥0.75, excellent; 0.40–0.75, good; and <0.40, poor. A P value of less than 0.05 was considered to indicate a statistically significant difference.

Results

Study population

Patient characteristics are summarized in *Table 1*. No

Table 2 Objective evaluation of the CT DICOM data

Index	Group A (n=28)	Group B (n=32)	Group C (n=30)
Jawbone (HU)	924.3±129.3	1,170.5±150.9[ab]	915.5±120.8
Masseter muscle (HU)	64.7±8.3	63.6±8.2	65.1±8.6
Background noise (SD)	11.3±2.6	13.8±2.9[ab]	12.5±2.3
SNR	81.1±13.8	84.6±14.7	78.2±15.6
CNR	79.9±14.3	80.2±12.6	80.0±13.9

Data are presented as mean ± standard deviation. P value after Bonferroni correction for multiple comparisons (P=0.05/3≈0.017). Group A, conventional CT dose 3D printing group; Group B, low-CT dose 3D printing group; Group C, 3D-CT control group. [a], Group B *vs.* Group A, P<0.017; [b], Group B *vs.* Group C, P<0.017. CT, computed tomography; DICOM, digital imaging and communications in medicine; HU, Hounsfield unit; SD, standard deviation; SNR, signal-to-noise ratio; CNR, contrast-to-noise ratio; 3D, three-dimensional.

Table 3 Comparison of objective indexes

Index	Group A (n=28)	Group B (n=32)	Group C (n=30)
$CTDI_{vol}$ (mGy)	17.3±0.1	7.1±0.6[ab]	19.5±0.8
DLP (mGy·cm)	356.5±24.2	142.7±20.3[ab]	368.2±22.4
ED (mSv)	0.8±0.1	0.3±0.1[ab]	0.9±0.3

Data are presented as mean ± standard deviation. P value after Bonferroni correction for multiple comparisons (P=0.05/3≈0.017). Group A, conventional CT dose 3D printing group; Group B, low-CT dose 3D printing group; Group C, 3D-CT control group. [a], Group B *vs.* Group A, P<0.017; [b], Group B *vs.* Group C, P<0.017. $CTDI_{vol}$, computed tomography dose index volume; DLP, dose-length product; ED, effective dose; CT, computed tomography; 3D, three-dimensional.

Table 4 Subjective scores of maxillofacial bone 3D printing quality

Index	Group A (n=28)	Group B (n=32)	P value
Clarity	3.3±0.5	3.4±0.5	0.442
Integrity	3.6±0.5	3.5±0.3	0.352
Accuracy	3.4±0.8	3.5±0.5	0.564
Artefacts	3.9±0.4	3.8±0.4	0.337

Data are presented as mean ± standard deviation. Group A, conventional CT dose 3D printing group; Group B, low-CT dose 3D printing group. CT, computed tomography; 3D, three-dimensional.

significant differences were observed in age, height, weight, body mass index (BMI), or class III malocclusion type between Groups A, B, and C (all P>0.05).

Objective evaluation

The CT [Hounsfield unit (HU)] of the jawbone and the SD value of Group B were greater than those of Groups A and C (*Table 2*, all P<0.017). Moreover, there was no statistically significant difference in the SNR or CNR among Groups A, B, and C.

Radiation dose

The CTDIvol, DLP, and ED in Group B (7.1±0.6 mGy, 142.7±20.3 mGy·cm and 0.3±0.1 mSv, respectively) were significantly lower than those in Group A and Group C (17.3±0.1 mGy, 356.5±24.2 mGy·cm, and 0.8±0.1 mSv; 19.5±0.8 mGy, 368.2±22.4 mGy·cm, and 0.9±0.3 mSv) (all P<0.001) (*Table 3*).

Subjective evaluation

Two maxillofacial surgeons subjectively scored the maxillofacial bone 3D printing quality in Groups A and B. The results revealed no significant differences between Groups A and B in terms of clarity, integrity, accuracy, or artefacts (P>0.05) (*Table 4*, *Figure 3*). The subjective consistency of the two maxillofacial surgeons was good, with a kappa value of 0.626. There were no significant difference in 3D modelling quality or 3D printing quality between the two groups with the naked eye (*Figures 4,5*).

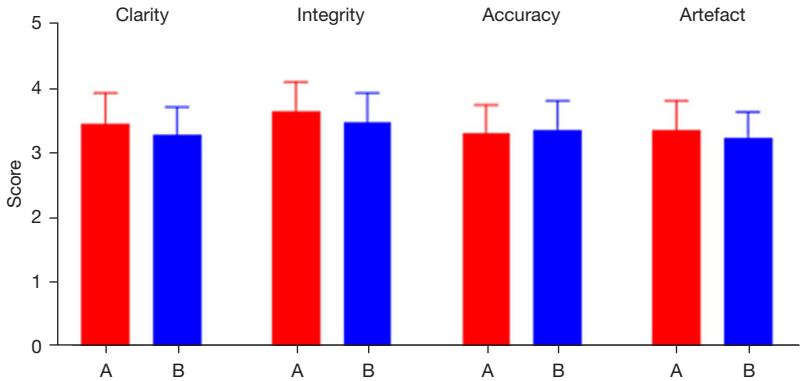

Figure 3 Comparison of subjectively evaluated maxillofacial bone 3D printing quality between Group A and Group B. Group A, conventional CT dose 3D printing group; Group B, low-CT dose 3D printing group. There were no significant differences between Groups A and B in terms of clarity, integrity, accuracy, or artefacts. CT, computed tomography; 3D, three-dimensional.

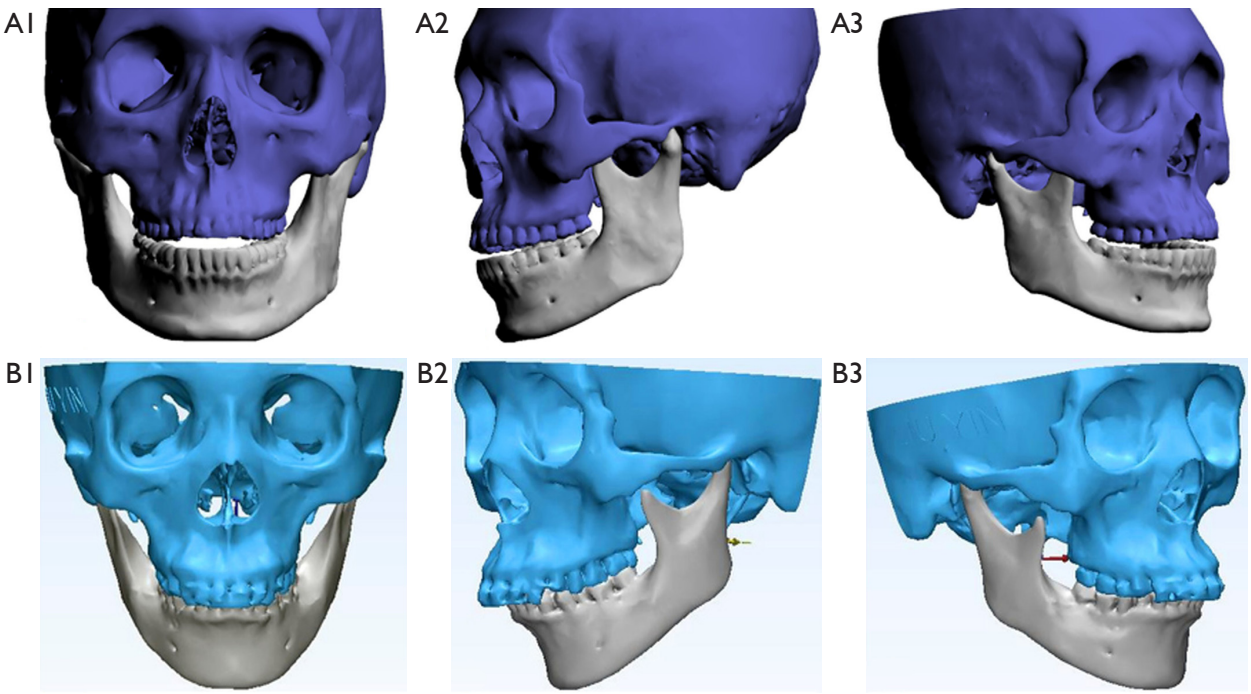

Figure 4 Comparison of the maxillofacial bone 3D modelling quality between Group A and Group B. (A1-A3) Group A scheme with 3D modelling. (B1-B3) Group B scheme finished 3D modelling. The results show that the 3D modelling qualities of Group A and Group B are not obviously different. Group A, conventional CT dose 3D printing group; Group B, low-CT dose 3D printing group. CT, computed tomography; 3D, three-dimensional.

Clinical application value

Six maxillofacial surgeons with different levels of seniority were selected to subjectively score the clinical value of maxillofacial bone 3D printing and 3D-CT reconstruction technology in class III malocclusion, including diagnosing and classifying, formulating a surgical plan, simulating the surgical process, and predicting postoperative recovery. The results revealed significantly higher subjective scores for the clinical value of Group A and Group B than those of Group C (all

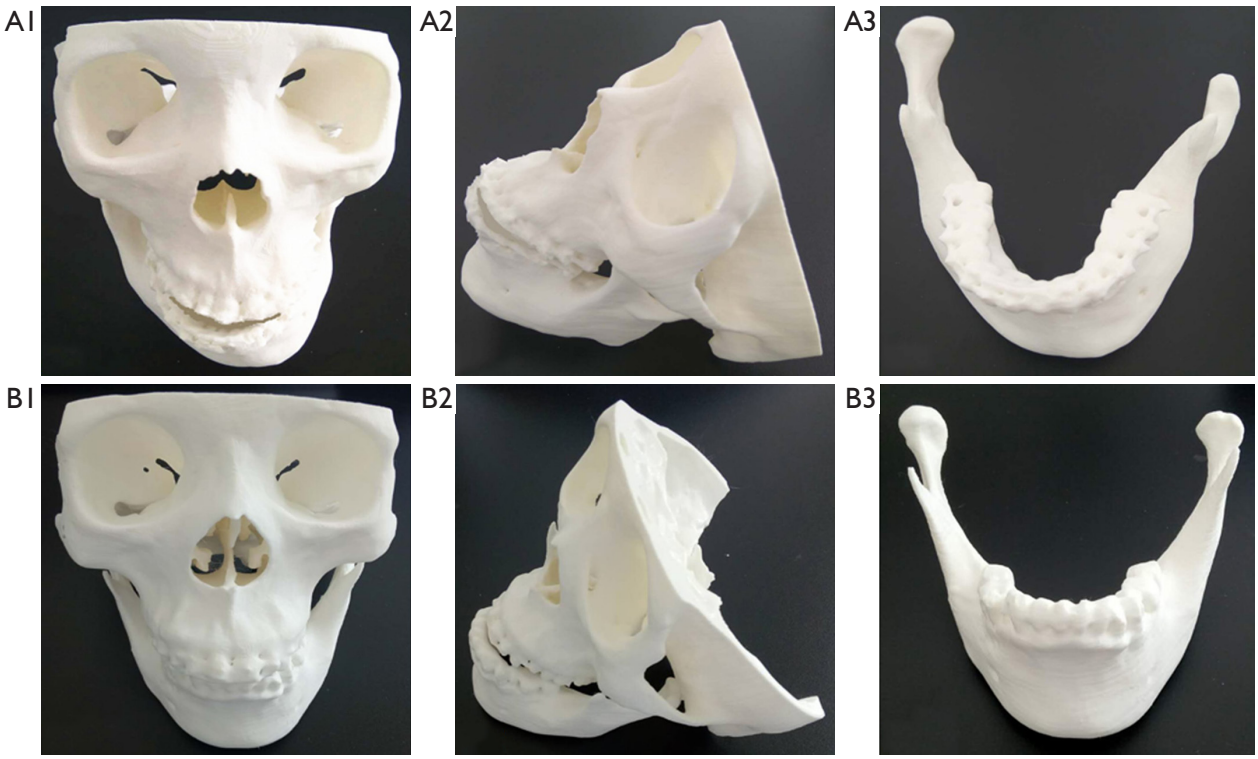

Figure 5 Comparison of the maxillofacial bone 3D printing quality between Group A and Group B. (A1-A3) Group A scheme finished 3D printing. (B1-B3) Group B scheme finished 3D printing. The results show that the 3D printing quality of Group A and Group B is not obviously different. Group A, conventional CT dose 3D printing group; Group B, low-CT dose 3D printing group. CT, computed tomography; 3D, three-dimensional.

Table 5 Subjective evaluation of the clinical application

Index	Group A (n=28)			Group B (n=32)			Group C (n=30)		
	Primary	Middle	Senior	Primary	Middle	Senior	Primary	Middle	Senior
(I)	4.4±0.5	3.9±0.4	4.0±0.5	4.2±0.6	4.0±0.4	3.8±0.6	2.9±0.5[ab]	3.1±0.5[ab]	3.3±0.5[ab]
(II)	4.3±0.6	3.8±0.5	3.8±0.5	4.4±0.4	4.0±0.4	3.7±0.4	2.9±0.4[ab]	3.1±0.3[ab]	3.3±0.5[ab]
(III)	4.2±0.4	4.0±0.4	3.9±0.5	4.3±0.5	4.0±0.6	3.8±0.4	2.7±0.5[ab]	2.9±0.4[ab]	3.0±0.4[ab]
(IV)	4.3±0.5	4.0±0.4	3.9±0.5	4.4±0.5	3.8±0.4	3.7±0.6	2.8±0.4[ab]	3.0±0.5[ab]	3.1±0.3[ab]

Data are presented as mean ± standard deviation. P value after Bonferroni correction for multiple comparisons (P=0.05/3≈0.017). (I) diagnosing and classifying; (II) formulating the surgical plan; (III) simulating the surgical process; (IV) predicting postoperative recovery. Group A, conventional CT dose 3D printing group; Group B, low-CT dose 3D printing group; Group C, 3D-CT control group. Group A *vs.* Group B, P>0.017. [a], Group C *vs.* Group A, P<0.017; [b], Group C *vs.* Group B, P<0.017. CT, computed tomography; 3D, three-dimensional.

P<0.05) (*Table 5*). Additionally, the subjective consistency of primary, middle, and senior surgeons was good, with kappa values of 0.676, 0.579 and 0.527, respectively. *Figure 6* shows the application of low-dose maxillofacial bone 3D printing technology in class III malocclusion correction.

Discussion

Maxillofacial bone 3D printing technology enables surgeons to obtain anatomical information more intuitively and accurately. In the present study, we adopted low-dose CT technology for maxillofacial bone 3D printing.

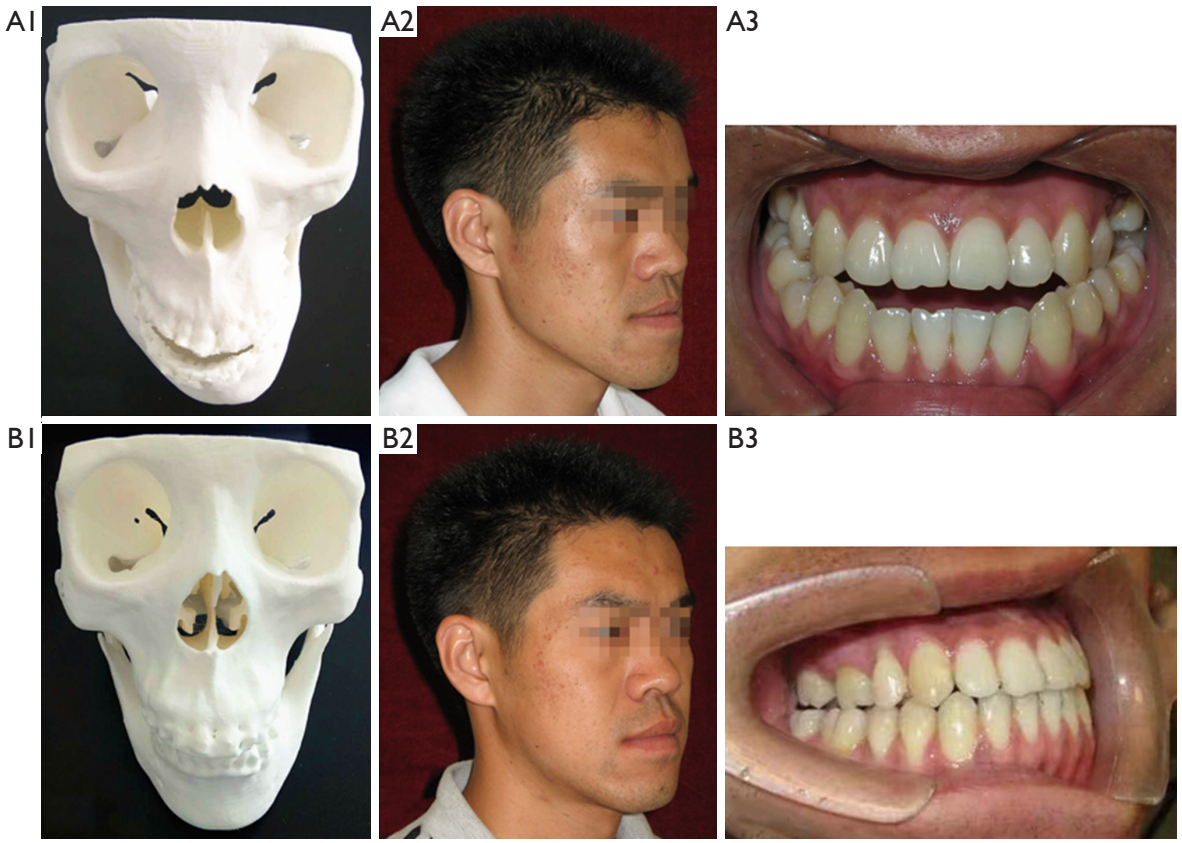

Figure 6 The application of low-dose maxillofacial bone 3D printing technology in class III malocclusion correction. (A1) Preoperative low-dose maxillofacial bone 3D printing; (A2) preoperative image of the patient; (A3) preoperative dental image. (B1) Postoperative low-dose maxillofacial bone 3D printing; (B2) postoperative image of the patient; (B3) postoperative dental image. Images (A2) and (B2) were published with the patient's consent. 3D, three-dimensional.

The radiation dose in the low-dose maxillofacial bone 3D printing group (0.3±0.1 mSv) was reduced by approximately 63% compared with that in the conventional-dose maxillofacial bone 3D printing group (0.8±0.1 mSv), and there were no significant differences in maxillofacial bone 3D printing quality between the two groups ($P>0.05$).

The radiation dose is proportional to the square of the tube voltage and directly proportional to the tube current (11). Reducing the tube voltage or tube current leads to an increase in image noise (12). In our study, there was no significant difference in the quality of 3D printing. The main reason is the compensation effect of the ASiR algorithm. The ASiR algorithm is a hybrid algorithm that uses the image obtained via FBP as the basis for iterative reconstruction to optimize image quality. The ASiR algorithm can reduce the CT radiation dose by 32–65% without substantially affecting image quality. In accordance with previous research, we selected 50% ASiR for quality compensation (13). Moreover, ATCM technology can automatically adjust the tube current according to the thicknesses of different tissues. ATCM technology can reduce the CT radiation dose by 15–50% (14,15).

Class III malocclusions can be divided into three types, and different types have different treatment methods. Intraoral sagittal split ramus osteotomy is used to treat type I patients. LeFort type I osteotomy before bilateral mandibular osteotomy is used to treat type II patients. Anterior mandibular subapical osteotomy is used for retraction, along with orthodontic treatment for type III patients. Maxillofacial bone 3D printing technology can display different types of malocclusions, and it is helpful for establishing a treatment plan (16). In our study, we demonstrated that maxillofacial bone 3D printing is significantly better than 3D-CT alone in diagnosing and

classifying, formulating a surgical plan, simulating the surgical process, and predicting postoperative recovery. On average, it would seem that the senior doctors gave higher scores in group C and lower scores in Groups A and B than did the doctors without as much experience (though this was not statistically tested). This would make sense, as seniors usually have a better understanding of anatomy and diseases even without 3D-printed models.

3D modelling is the last step before 3D printing, excluding elements of 3D printing technology, such as the 3D printing process, operator proficiency and other factors. The quality of 3D modelling can directly affect the quality of 3D printing (17). Effective 3D modelling can avoid wasting materials and time. In our study, it took approximately 1 hour to complete maxillofacial bone 3D modelling and approximately 20 hours to complete maxillofacial bone 3D printing. Recently, cone-beam CT (CBCT) has become popular and can also be used for 3D printing (18). However, we found that CBCT has limitations in terms of the scanning range and anatomical integrity (19,20). Most nondental specialized hospitals do not have CBCT devices installed. Therefore, in this study, we selected the general body spiral CT for this experiment.

We acknowledge some limitations to our study. First, the sample size was very small. Second, we did not assess the effects of other iterative reconstruction algorithms [such as model-based iterative (MBIR) and artificial intelligence-based reconstructions] or different iterative weights. Third, this study lacked comparisons with CBCT. Fourth, this study focused only on the CT DICOM data because of its effect on 3D printing quality and did not consider other variables, such as 3D printing methods, materials, software, and technician proficiency. Fifth, there has been no discussion on whether maxillofacial bone 3D printing technology is more effective than 3D-CT in improving clinical diagnosis and treatment. Finally, we did not perform a relevant measurement analysis of class III malocclusion. Further research should be performed in these areas.

Conclusions

Low-dose CT technology can be effectively applied for maxillofacial bone 3D printing and reduces the radiation dose without affecting the quality of 3D printing. Furthermore, we demonstrated that the clinical application value of maxillofacial bone 3D printing in class III malocclusion, especially in diagnosing and classifying, formulating a surgical plan, simulating the surgical process, and predicting postoperative recovery, was better than that of 3D-CT technology.

Acknowledgments

Funding: This study was supported by the Nanjing Drum Tower Hospital Clinical Research Special Fund, China (No. 2024-LCYJ-MS-27).

Footnote

Reporting Checklist: The authors have completed the GRRAS reporting checklist. Available at https://qims.amegroups.com/article/view/10.21037/qims-22-1266/rc

Conflicts of Interest: All authors have completed the ICMJE uniform disclosure form (available at https://qims.amegroups.com/article/view/10.21037/qims-22-1266/coif). Y.X.J.W. serves as the Editor-in-Chief of *Quantitative Imaging in Medicine and Surgery*. The other authors have no conflicts of interest to declare.

Ethical Statement: The authors are accountable for all aspects of the work in ensuring that questions related to the accuracy or integrity of any part of the work are appropriately investigated and resolved. The study was conducted in accordance with the Declaration of Helsinki (as revised in 2013). Ethical approval for this research was obtained from the Ethics Committee of Jinling Hospital, Affiliated Hospital of Medical School, Nanjing University, China (No. 2022DZGZR-075), and all patients provided informed consent.

References

1. Peng J, Jiang Y, Shang F, Yang Z, Qi Y, Chen S, Yang Y, Jiang R. Changes in masseter muscle morphology after surgical-orthodontic treatment in patients with skeletal

Class III malocclusion with mandibular asymmetry: The automatic masseter muscle segmentation model. Am J Orthod Dentofacial Orthop 2024;165:638-51.
2. De Ridder L, Aleksieva A, Willems G, Declerck D, Cadenas de Llano-Pérula M. Prevalence of Orthodontic Malocclusions in Healthy Children and Adolescents: A Systematic Review. Int J Environ Res Public Health 2022;19:7446.
3. Li Z, Hung KF, Ai QYH, Gu M, Su YX, Shan Z. Radiographic Imaging for the Diagnosis and Treatment of Patients with Skeletal Class III Malocclusion. Diagnostics (Basel) 2024;14:544.
4. Martins FAG, Motta AR, Neves LS, Furlan RMMM. Evaluation of the maximum tongue and lip pressure in individuals with Class I, II, or III Angle malocclusions and different facial types. Codas 2023;35:e20220102.
5. Chrz K, Bruthans J, Ptáčník J, Štuka Č. A Cost-Affordable Methodology of 3D Printing of Bone Fractures Using DICOM Files in Traumatology. J Med Syst 2024;48:66.
6. Xiao M, Zhang M, Lei M, Hu X, Wang Q, Chen Y, Ye J, Xu R, Chen J. Application of ultra-low-dose CT in 3D printing of distal radial fractures. Eur J Radiol 2021;135:109488.
7. Li G, Dong J, Cao Z, Wang J, Cao D, Zhang X, Zhang L, Lu G. Application of low-dose CT to the creation of 3D-printed kidney and perinephric tissue models for laparoscopic nephrectomy. Cancer Med 2021;10:3077-84.
8. Almeshari A, Abdelkarim AZ, Geha H, Khan AA, Ruparel N. Assessing the Efficacy of Planmeca ProMax® 3D Cone-Beam CT Machine in the Detection of Root Fractures With Varied Metal Artifact Reduction Settings and Three Kilovoltage Peak Levels. Cureus 2023;15:e35647.
9. Al-Ekrish AA, Alfadda SA, Tamimi D, Alfaleh W, Hörmann R, Puelacher W, Widmann G. Do Ultra-Low Multidetector Computed Tomography Doses and Iterative Reconstruction Techniques Affect Subjective Classification of Bone Type at Dental Implant Sites? Int J Prosthodont 2018;31:465-70.
10. Huang X, Zhao W, Wang G, Wang Y, Li J, Li Y, Zeng Q, Guo J. Improving image quality with deep learning image reconstruction in double-low-dose head CT angiography compared with standard dose and adaptive statistical iterative reconstruction. Br J Radiol 2023;96:20220625.
11. Li B, Wang X, Fan Y, Wang S, Tong X, Zhang J, Li J, Liu Y. Evaluation of BMI-based tube voltage selection in CT colonography: A prospective comparison of low kV versus routine 120 kV protocol. J Appl Clin Med Phys 2023;24:e13955.
12. Kawahara D, Toyoda T, Yokomachi K, Fujioka C, Nagata Y. Dose uncertainty due to energy dependence in dual-energy computed tomography. Pol J Radiol 2023;88:e270-4.
13. Widmann G, Bischel A, Stratis A, Kakar A, Bosmans H, Jacobs R, Gassner EM, Puelacher W, Pauwels R. Ultralow dose dentomaxillofacial CT imaging and iterative reconstruction techniques: variability of Hounsfield units and contrast-to-noise ratio. Br J Radiol 2016;89:20151055.
14. Sookpeng S, Martin CJ. Impact of iodinated contrast media concentration on image quality for dual-energy CT and single-energy CT with low tube voltage settings. Acta Radiol 2023;64:1047-55.
15. de Camargo GE, Carneiro GN, Real JV, Doro RB, Malthez ALMC. Development of phantom for current modulation quality assurance test on computed tomography. Radiat Prot Dosimetry 2023;199:1029-33.
16. Kim M, Li J, Kim S, Kim W, Kim SH, Lee SM, Park YL, Yang S, Kim JW. Individualized 3D-Printed Bone-Anchored Maxillary Protraction Device for Growth Modification in Skeletal Class III Malocclusion. J Pers Med 2021;11:1087.
17. Domínguez-Robles J, Shen T, Cornelius VA, Corduas F, Mancuso E, Donnelly RF, Margariti A, Lamprou DA, Larrañeta E. Development of drug loaded cardiovascular prosthesis for thrombosis prevention using 3D printing. Mater Sci Eng C Mater Biol Appl 2021;129:112375.
18. Lambrecht JT, Berndt DC, Schumacher R, Zehnder M. Generation of three-dimensional prototype models based on cone beam computed tomography. Int J Comput Assist Radiol Surg 2009;4:175-80.
19. Alshomrani F. Cone-Beam Computed Tomography (CBCT)-Based Diagnosis of Dental Bone Defects. Diagnostics (Basel) 2024;14:1404.
20. Lechner W, Kanalas D, Haupt S, Zimmermann L, Georg D. Evaluation of a novel CBCT conversion method implemented in a treatment planning system. Radiat Oncol 2023;18:191.

Cite this article as: Miao Q, Li G, Wáng YXJ, Wang J, Wang H, Chen W, Shao Y. Feasibility study of low-dose computed tomography (CT) technology for maxillofacial bone three-dimensional (3D) printing in skeletal class III malocclusion. Quant Imaging Med Surg 2024;14(12):8238-8248. doi: 10.21037/qims-22-1266

